

Remote-Controlled Peristaltic Locomotion in Free-Floating PNIPAM Hydrogels

Jarod Gregory,¹ M. Sadegh Riasi,¹ Jonathan Cannell,¹ Hitesh Arora,² Lilit Yeghiazarian,¹ Vasile Nistor¹

¹Department of Biomedical, Chemical, and Environmental Engineering, University of Cincinnati, Cincinnati, Ohio 45220

²HGST, a Western Digital company, 3403 Yerba Buena Rd., San Jose CA, 95135

Correspondence to: L. Yeghiazarian (E-mail: lilit.yeghiazarian@uc.edu) and V. Nistor (E-mail: vasile.nistor@uc.edu)

ABSTRACT: Peristalsis-driven locomotion, by nature of its flexibility and deformability, is a highly advantageous mechanism for mobility in soft materials and robots; however, utilization of this mechanism has been limited to restricted, frictional environments. (Seok et al., presented at 2010 IEEE International Conference on Robotics and Automation, Anchorage, AK May 3–8, 2010; Boxerbaum et al., *Int J Robotics Res* 2012, 31, 302; Boxerbaum et al., presented at 2011 IEEE/RSJ International Conference on Intelligent Robots and Systems, San Francisco, CA, 2011; Arora et al., *J Polym Sci Part A: Polym Chem* 2009, 47, 5027). We have removed this limitation and expanded the use of peristaltic locomotion to open aqueous environments by remotely inducing peristalsis via spatially controlled volume phase transitions in thermosensitive poly(*N*-isopropylacrylamide) (PNIPAM) hydrogels. The resulting asymmetry causes steady, incremental linear displacement in the hydrogel's center of mass, thus producing directed, remote-controlled locomotion. In our proof-of-principle system, we controlled the peristaltic locomotion of the hydrogels using a handheld laser to selectively induce volume phase transitions in the hydrogel. The PNIPAM hydrogels' energy absorbance capability was enhanced by incorporating the New Indocyanine Green laser dye (IR-820) into the gel. The use of IR-820 is likely to expand the application space for these hydrogels due to new opportunities for conjugation chemistry. (Prajapati et al., *Molecular Imaging* 2009, 8, 45; Fernandez-Fernandez et al., *Molecular Imaging* 2011, 11, 1). Overall, such an approach increases the capability of both peristaltic locomotion as a mechanism for mobility in soft robots, and PNIPAM hydrogels as a biotechnological platform. © 2014 Wiley Periodicals, Inc. *J. Appl. Polym. Sci.* 2014, 131, 40927.

KEYWORDS: biomimetic; functionalization of polymers; gels; hydrophilic polymers

Received 25 February 2014; accepted 19 April 2014

DOI: 10.1002/app.40927

INTRODUCTION

Biomimetic devices take advantage of nature's ability to perform specific functions or utilize specific features.¹ Nature displays a plethora of mechanisms for locomotion,² including peristaltic locomotion exhibited by earthworms that has been studied in the field of soft robotics in recent years.^{1–13} Through a number of differing methods, robots have been able to reproduce the three essential components of earthworm-inspired motion: engagement, propulsion, and detachment.¹⁴ In these processes, the robots (or the earthworms that inspired this technique) engage with a frictional surface, propel forward, and detach from the frictional surface as a means of displacement. Segmented and single-bodied soft robots are becoming increasingly popular,⁶ as these devices are capable of utilizing peristaltic motion as a mechanism for movement while retaining the flexible and deformable structure that allows an earthworm to be versatile in crawling and burrowing actions within frictional environments.^{3–6} Our proof-of-principle system expands the

potential functional environments of mobile soft robots that utilize peristaltic motion to open aqueous environments, thus extending the usage of these robots for existing applications and creating new opportunities for the field of soft robotics.

The use of peristaltic motions as a means for transport is a familiar topic in the more narrow study of hydrogels as functional soft materials.^{8–12} For example, the Belousov–Zhabotinsky reaction, a pulsating, far-from-equilibrium reaction,⁷ has been utilized to induce cyclical peristaltic motion in hydrogels, which enabled the transport of objects inside the inner diameter of a hollow tubular hydrogel, thus mimicking an esophagus or intestine.^{8–12} These hydrogels are stationary, as only the transported object is mobilized from the peristaltic motion.

In our previous work, thermosensitive cylindrical hybrid poly(*N*-isopropylacrylamide) (PNIPAM) hydrogels were shown to be capable of peristaltic locomotion within a frictional capillary tube.^{6,13,15} These hydrogels use a Laponite derivative as a

Additional Supporting Information may be found in the online version of this article.

© 2014 Wiley Periodicals, Inc.

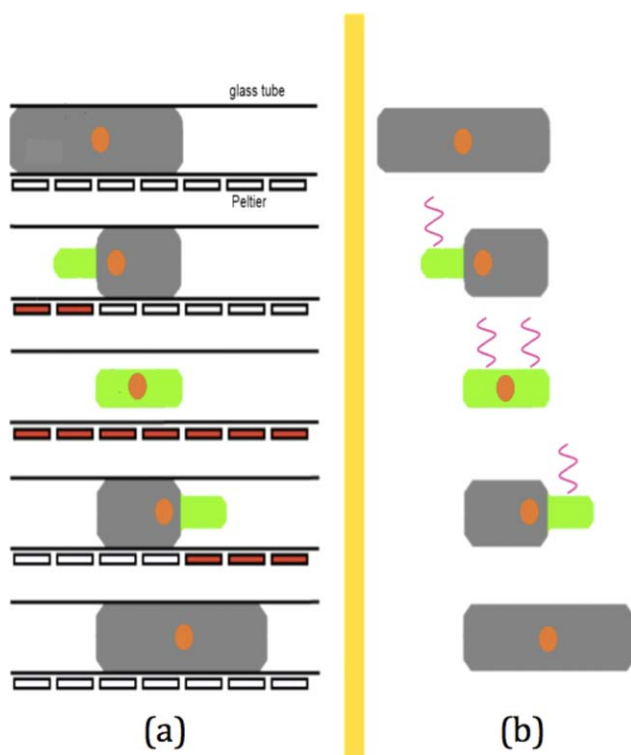


Figure 1. (a) Representation of the mechanism for movement of a hydrogel in a capillary tube, as done by Yeghiazarian et al.^{6,13,15} The center of mass is indicated by the red dot. The selective heating was performed by Peltier elements, and peristaltic locomotion is performed in a frictional environment. (b) Mechanism for our proof-of-principle system, where we rely on the shifting of the center of mass of the hydrogel resulting from asymmetry caused by a laser-induced volume phase transition. As water is expelled due to volume phase transition, the center of mass shifts as represented in the figure. The red curved lines indicate heat absorption from a handheld laser. [Color figure can be viewed in the online issue, which is available at wileyonlinelibrary.com.]

cross-linker in their chemical structure, which increases their mechanical stability.¹⁵ They undergo a volume phase transition at approximately 32°C,² during which their volume can shrink by as much as several hundred times the original synthesized structure.¹³ By spatially controlling volume phase transitions along the hydrogel, we were able to induce the necessary asymmetry to generate peristaltic locomotion within a tube. In our past experiments, volume phase transitions were induced by selectively heating the capillary tube and the hydrogel inside using stationary Peltier elements as shown in Figure 1(a).² Figure 1(b) illustrates our current proof-of-principle system, in which we sought to enable remote-controlled peristaltic locomotion in an open environment. We achieved this by (1) functionalizing our hybrid hydrogel with a dye that could absorb energy from a laser and (2) using a handheld laser to selectively irradiate the gel and induce volume phase transitions remotely in a manner that mimics peristaltic motion. Each shrinking and swelling cycle produces a small, albeit significant and reproducible displacement of the center of mass of the hydrogel, resulting in overall translation of the hydrogel. Details of these experiments are described below.

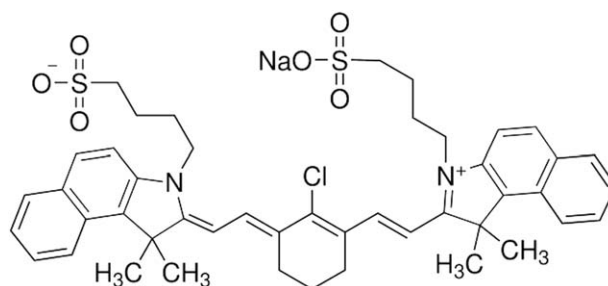


Figure 2. Chemical structure of IR-820.

Hybrid hydrogels have been shown to effectively adsorb cationic solutes out of solution.¹⁶ The IR-820 dye used in this study contains both positive and negative charges (Figure 2). The positive quaternary ammonium group binds to the Laponite cross-linker in the hybrid hydrogels chemical structure, creating a mechanism for dye adsorption to the hydrogel.¹⁶ The adsorption occurs rapidly, concentrating the dye on and near the circumference of the hydrogel.¹⁶ Figure 3 shows a cross section of a cylindrical hybrid hydrogel of approximately 5 mm in diameter, on which it is clear that only the area near the surface of the hydrogel has adsorbed the dye. The dye molecules that were directly adsorbed on to or within the hydrogel effectively stayed bound to the hydrogel. Figure 4(a) shows the hydrogel before 10 full heat-induced phase changes, while Figure 4(b) shows the hydrogel after the phase changes. There was no noticeable expulsion of IR-820 molecules during the phase changes.

Volume phase transitions in PNIPAM hydrogels have been remotely induced via lasers,¹⁷ although not in the context of locomotion. With the adsorption of IR-820 into our hydrogel, we were able to use an 830-nm handheld laser to quickly and selectively induce volume phase transitions in a floating cylindrical hydrogel. Clearly, the amount of dye adsorbed at the rim of the gel suffices to absorb enough energy from the laser to induce volume phase transitions. On average, the hydrogel shrank by 6.5% (+/-1.5%) radially and by 1.5% (+/-0.75%) linearly as a result of the volume phase transition. This shrinkage was sufficient in creating the asymmetry necessary for a shift in center of mass and linear movement by the hydrogel in an open environment. Our hydrogels displaced in a linear direction by a distance of 11% (+/-3.5%) of the initial lengths over one cycle. A video of a typical experiment can be found in Supporting Information. Two methods of video analysis of the linear displacement of our hydrogels are detailed below.

Figure 5(a) shows a floating hydrogel in its initial position. The red markers indicate the initial positions of each end of the hydrogel for reference throughout the volume phase transition cycle. Figure 5(b) shows the hydrogel undergoing a laser-induced volume phase transition on its left end; the area targeted by the laser appearing opaque. As evident in the figure, the phase transition side of the hydrogel is shrinking towards its center as the right end stays relatively still. As water is expelled from the hydrogel in the area of the volume phase transition, its center of mass is moving toward the right side of the figure. This is the driving force of the linear displacement of the hydrogel [see Figure 2(b)]. Figure 5(c) shows the continued propagation of both the volume

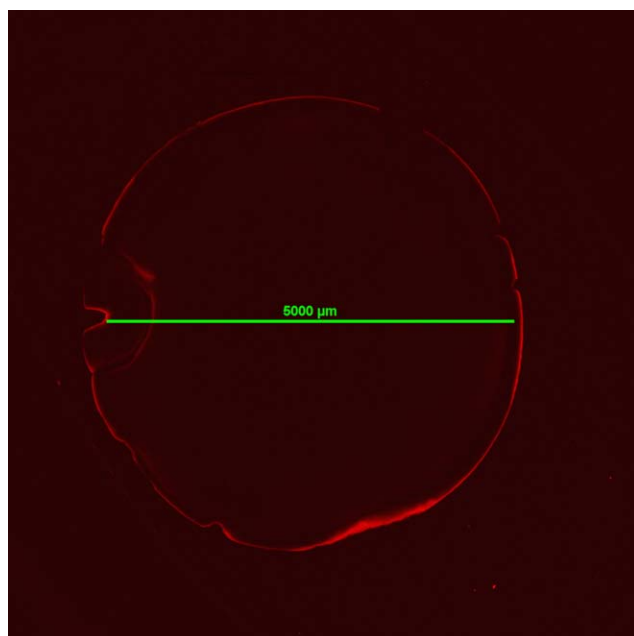


Figure 3. Image of a cross section of a cylindrical PNIPAM hydrogel that has adsorbed IR-820 dye being excited with an 820-nm laser. This image shows the nature of the IR-820's adsorption, which is localized along the surface of the hydrogel. [Color figure can be viewed in the online issue, which is available at wileyonlinelibrary.com.]

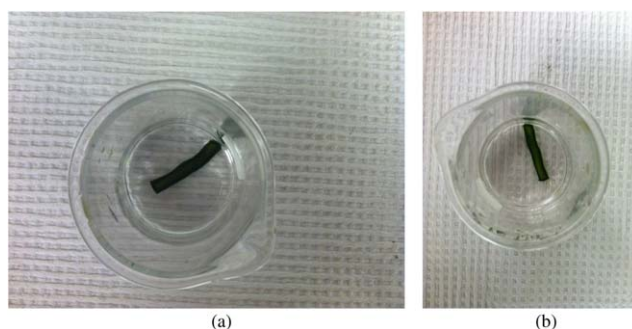


Figure 4. (a) Cylindrical hydrogel that has adsorbed IR-820 dye and has been placed in 20 mL of clean distilled water. (b) Same hydrogel after 10 full heat-induced phase changes. The hydrogel effectively retains all adsorbed dye. [Color figure can be viewed in the online issue, which is available at wileyonlinelibrary.com.]

phase transition from left to right along the length of the hydrogel, as well as its continued displacement. At this instant in the cycle, the volume phase transition has surpassed the midpoint of the gel and the right end of the hydrogel has begun to displace toward the right side of the figure. Finally, Figure 5(d) shows the final position of the hydrogel. After one 24.5 s-long volume phase transition cycle, the hydrogel has displaced approximately 2.1 mm, or 7.9% of its original length of 26.5 mm.

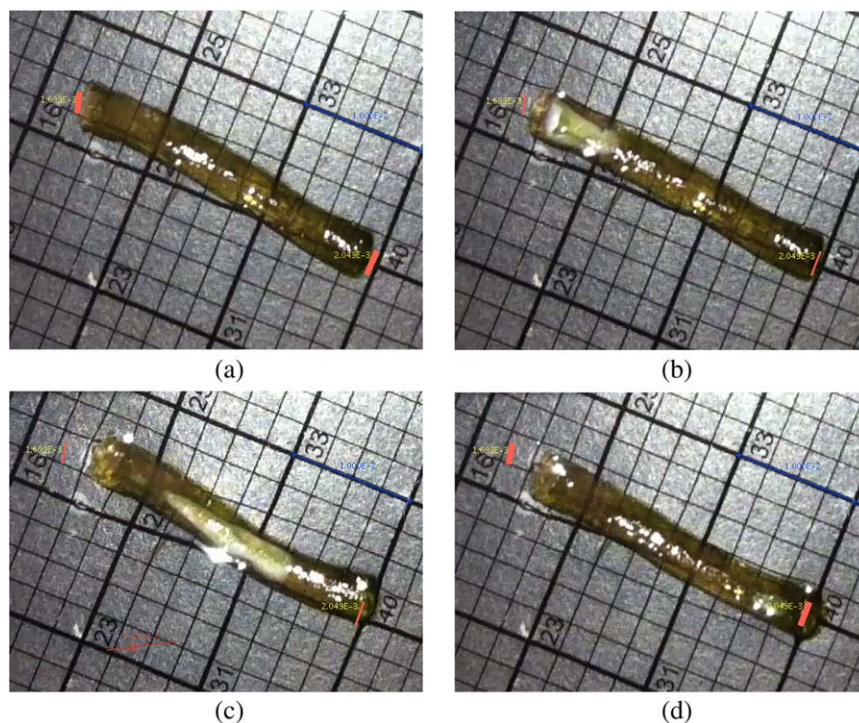


Figure 5. Floating hybrid hydrogel functionalized with IR-820 laser dye with a linear displacement of 2.11 mm via linear and radial shrinkage caused by a volume phase transition induced by laser. The initial end-markers stay fixed throughout analysis. (a) Hydrogel is at its initial position and has an initial length of 26.5 mm. (b) Hydrogel is undergoing laser-induced volume phase transition on its left end. At $t = 6.5$ s, the hydrogel's left end has displaced 0.5 mm while the right end has displaced 0.2 mm. At this moment, the linear shrinkage is 1.3% and radial shrinkage is 4.5% at the area of volume phase transition. (c) At $t = 13.5$ s, the volume phase transition has progressed to the middle of the hydrogel. The displacement of the left end is 2.3 mm and the displacement of the right end is 1.7 mm. The radial shrinkage at the area of volume phase transition is 5.2%. Finally, (d) shows the hydrogel at $t = 24.5$ s. The left end has displaced 2.3 mm while the right end has displaced 1.9 mm. At this final location, the left end has a larger displacement from its initial position than the right end. The displacement of the two ends will average out with time as full rehydration occurs. [Color figure can be viewed in the online issue, which is available at wileyonlinelibrary.com.]

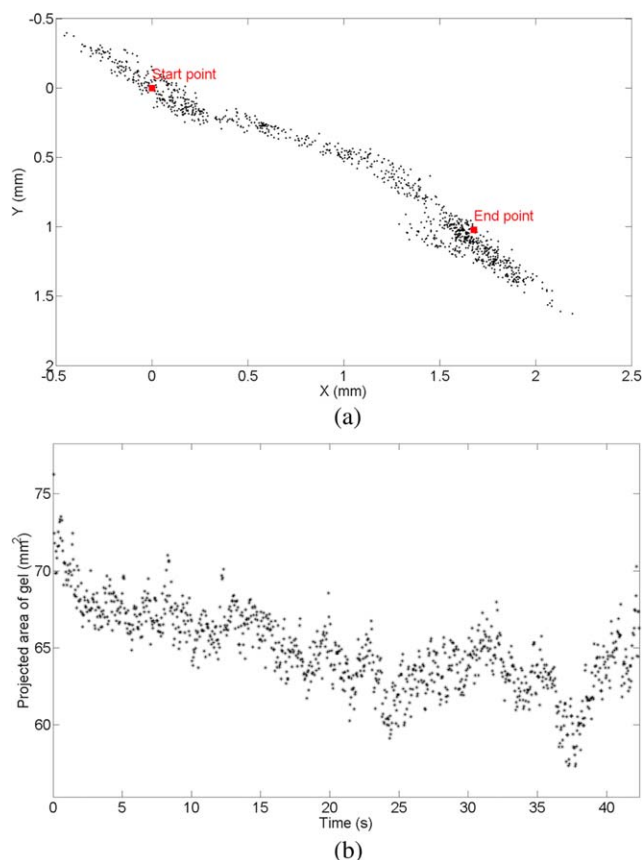


Figure 6. (a) Movement of the geometric centroid of a hydrogel undergoing a volume phase transition cycle. The hydrogel displaces linearly by 1.96 mm, which was 9.9% of the initial gel length of 19.8 mm. The movement is not absolutely linear due to heating of surrounding water and asymmetrical heating of one side of the hydrogel, causing the center of mass to move slightly sideways. (b) Projected two-dimensional area of the gel as it goes through one volume phase transition cycle. The oscillatory nature of the projected two-dimensional area is due to changes in size of the gel during the cycle, as well as a nonuniform pace of heating with the laser. If the laser moves from end-to-end faster on one portion of the hydrogel than the portion before, or if the laser is inadvertently heating the surrounding water, the hydrogel begins to regain a portion of its original size. [Color figure can be viewed in the online issue, which is available at wileyonlinelibrary.com.]

A control system without the laser dye was set up to mimic the system displayed in Figure 5. In the control system, the hydrogel showed no physical signs of an induced volumetric phase change when exposed to the laser and, consequently, was not displaced.

Figure 6(a) shows the linear displacement of the hydrogel on the x - y plane through tracking of the geometric centroid of the projected two-dimensional area of the gel, as it undergoes a single volume phase transition cycle. This method provides a systematic means of measuring displacement. As the figure shows, the hydrogel's movement is not strictly linear. The handheld laser can lead to nonuniform radial heating caused by hand tremor and absorption of energy from the laser by the surrounding water, in which case the center of mass will shift slightly toward one side of the hydrogel as well as from one end to the other. Fluid flow around the gel caused by temperature gradient in the surrounding liquid during laser heating can also lead to minor shifts in the position of the gel.

Figure 6(b) shows changes in the projected two-dimensional area of the hydrogel as the volume phase transition propagates linearly through the gel. The oscillatory pattern is due to fluctuations in the size of the gel during the cycle, as well as high-frequency segmentation errors in image processing. The nonuniform heating pattern due to manual control of the laser is another contributor to this dynamic. For example, if the laser heats one portion of the hydrogel for less time than the previous portion, the hydrogel will begin to regain some of its original size. Absorption of heat from the laser by surrounding water at various times throughout the process can also cause the nonuniform heating. At the end of the volume phase transition cycle, the hydrogel regains nearly its entire original size in approximately 5s.

To the best of our knowledge, this is the first system to experimentally produce remote-controlled locomotion in hydrogels. In doing so, our system became the first to extend locomotion via peristalsis for soft materials into open, unconstrained environments, which expands the potential applicability of similar soft materials.¹⁸ Mobility in hydrogels has ramifications as an environmental biosensor,¹⁹ as well as expanded capabilities in the area of targeted drug delivery,^{20,21} among others.²²

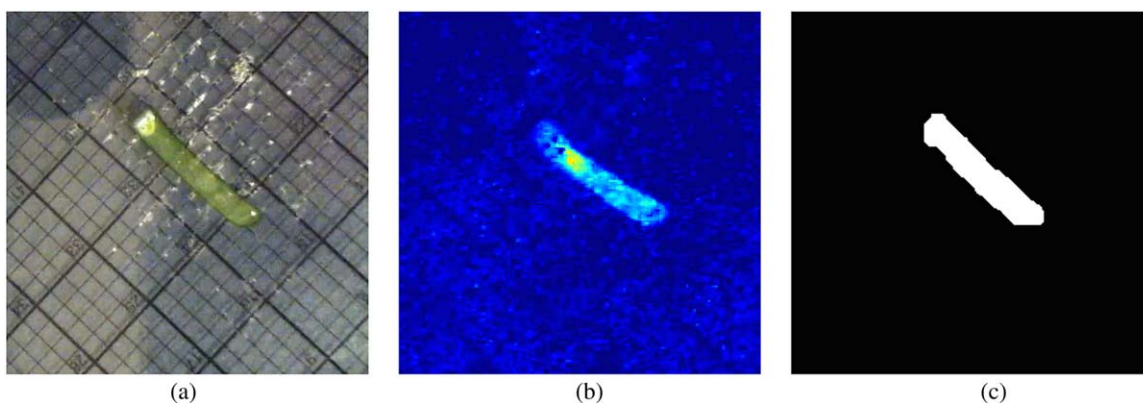


Figure 7. Stages of the image segmentation process: (a) original RGB video frame, (b) greenness map, and (c) the segmented video frame. [Color figure can be viewed in the online issue, which is available at wileyonlinelibrary.com.]

Generally, the field of soft robotics may benefit from the broadened circumstances in which peristaltic locomotion may be used.

In summation, we remotely induced a cycle of volume phase transitions in a hydrogel in a manner that mimics peristaltic motion and used that as a mechanism for directed locomotion in a free-floating PNIPAM hydrogel. We accomplished this by increasing the energy absorption capabilities of the hydrogel by allowing it to adsorb IR-820 laser dye and then selectively shrinking the gel with a handheld laser. This proof-of-principle system greatly expands the environments in which a mobile hydrogel can be functional, elaborating on the body of work on PNIPAM hydrogels and widening the applicability of soft robotics in the areas of environmental sensing and biotechnology. Our future work will focus on the optimization of this device.

EXPERIMENTAL

The PNIPAM hybrid hydrogels were synthesized as shown elsewhere.⁶ Laponite XLG (0.4 g, Southern Clay) was vigorously stirred in to 28.5 mL of distilled water until the water returns to clear (approximately 30 min). *n*-Isopropylacrylamide (3.5 g, Sigma-Aldrich) was added and stirred until dissolved (approximately 10 min). Potassium persulfate (30 mg, Sigma-Aldrich) was dissolved in 1.5 mL of distilled water and added to the solution, followed immediately by tetramethylethylenediamine (.024 mL, Sigma-Aldrich). Nine glass tubes of 1 mm inside diameter and varying lengths (1–4 cm) were submerged in the solution, and the polymerization was allowed to occur over 24 h at 50°C.

The glass tubes were silanized for hydrophobicity by submerging the glass tubes in a solution of distilled water, acetic acid (1.0% wt, Sigma-Aldrich), and diethoxydimethylsilane (5.0% wt, Sigma-Aldrich) and then dried for 30 min in a vacuum oven at 113°C.

The fluorescent image in Figure 3 was performed by a Nikon A1R Multiphoton system attached to a Nikon Eclipse FN1 Upright microscope. The laser used is a Coherent Chameleon Vision II Ti:Sapphire laser set to 820 nm. The objective was a 16X Nikon CFI Long Working Distance Achromatic Objective with a Numerical Aperture of 0.8 and a 3-mm working distance.

Volume phase transitions were induced with a handheld laser (WarnLaser, 1W, 830 nm). The laser was directed at a singular portion of the hydrogel for approximately 2 s, starting at one end of the hydrogel and moving to the other. As the hydrogel began to displace, the laser operator would follow the hydrogel to attempt to induce similar volume phase transition cycles throughout each trial.

The PNIPAM hybrid hydrogels adsorbed 2-[2-[2-chloro-3-[[1,3-dihydro-1,1-dimethyl-3-(4-sulfobutyl)-2H-benzo[e]indol-2-ylidene]ethylidene]-1-cyclohexen-1-yl]-ethenyl]-1,1-dimethyl-3-(4-sulfobutyl)-1H-benzo[e]indolium hydroxide inner salt sodium salt (IR-820, Sigma-Aldrich) by submerging the fully swollen hydrogels in various concentrations of IR-820 and distilled water solutions.

The video analysis in Figure 5 was performed using Tracker video analysis. For the kinetics analysis for Figure 6, we segmented the video frames recorded during the experiment. To

do this, we first applied Otsu's thresholding technique on the greenness map of each original RGB video frame,²³ using MatLab. The greenness map was generated by mapping the RGB image to an index image using a greenness measure (2*G-R-B). We then applied the sequence of morphological dilation, filling and erosion to get a smooth hydrogel geometry (Figure 7).

ACKNOWLEDGMENTS

This research was supported by the NSF CBET-1248385 and NSF CEAS AY-REU Program, Part of NSF Type-1 STEP Grant, Grant ID No.: DUE-0756921. The authors thank Ulrich Wiesner (Cornell University) for critical reading of the manuscript and the Confocal Imaging Core at Cincinnati Children's Hospital Medical Center.

REFERENCES

1. Yeghiazarian, L.; Lux, R. In *Phase Transitions in Cell Biology*, Pollack, G., Chin, W., Eds.; Springer: New York, NY, **2008**.
2. Mohammed, J. S.; Murphy, W. L. *Adv. Mater.* **2009**, *21*, 2361.
3. Seok, S.; Onal, C. D.; Wood, R.; Rus, D.; Kim, S. Presented at 2010 IEEE International Conference on Robotics and Automation, Anchorage, AK, May 3–8, **2010**.
4. Boxerbaum, A. S.; Shaw, K. M.; Chiel, H. J.; Quinn, R. D. *Int. J. Robotics Res.* **2012**, *31*, 302.
5. Boxerbaum, A. S.; Horchler, A. D.; Shaw, K. M.; Chiel, H. J.; Quinn, R. D. Presented at 2011 IEEE/RSJ International Conference on Intelligent Robots and Systems, San Francisco, CA, September 25–30, **2011**.
6. Arora, H.; Malik, R.; Yeghiazarian, L.; Cohen, C.; Wiesner, U. *J. Polym. Sci. Part A: Polym. Chem.* **2009**, *47*, 5027.
7. Epstein, I. R.; Pojman, J. A. *An Introduction to Nonlinear Chemical Dynamics*, Oxford University Press, New York, **1998**.
8. Maeda, S.; Hara, Y.; Yoshida, R.; Hashimoto, S. *Angew. Chem.* **2008**, *120*, 6792.
9. Yoshida, R.; Okano, T. In *Biomedical Applications of Hydrogels Handbook*, Ottenbrite, R. M., Park, K., Okano, T., Eds.; Springer: New York, **2010**.
10. Shiraki, Y.; Yoshida, R. *Angew. Chem.* **2012**, *124*, 6216.
11. Shinohara, S.; Seki, T.; Sakai, T.; Yoshida, R.; Takeoka, Y. *Chem. Commun. (Camb.)* **2008**, *39*, 4735.
12. Yoshida, R. *Adv. Mater.*, **2010**, *22*, 3463.
13. Yeghiazarian, L.; Arora, H.; Nistor, V.; Montemagno, C.; Wiesner, U. *Soft Matter* **2007**, *3*, 939.
14. Prajapati, S. I.; Martinez, C. O.; Bahadur, A. H. N.; Wu, I. Q.; Zheng, W.; Lechleiter, J. D.; Mcmanus, L. M.; Chisholm, G. B.; Michalek, J. E.; Shireman, P. K.; Keller, C. *Mol. Imaging* **2009**, *8*, 45.
15. Yeghiazarian, L.; Mahajan, S.; Montemagno, C.; Cohen, C.; Wiesner, U. *Adv. Mater.* **2005**, *17*, 1869.
16. Thomas, P. C.; Cipriano, B. H.; Raghavan, S. R. *Soft Matter* **2011**, *7*, 8192.
17. Tsuboi, Y.; Nishino, M.; Kitamura, N. *Polym. J.* **2008**, *40*, 367.

18. Kuksenok, O.; Balazs, A. C. *Adv. Funct. Mater.* **2013**, *23*, 4601.
19. Massad-Ivanir, N.; Shtenberg, G.; Zeidman, T.; Segal, E. *Adv. Funct. Mater.* **2010**, *20*, 2269.
20. Qiu, Y.; Park, K. *Adv. Drug Deliver. Rev.* **2001**, *53*, 321.
21. Gupta, P.; Vermani, K.; Garg, S. *Drug Discov. Today* **2002**, *7*, 569.
22. Otsu, N. *IEEE Trans. Syst. Man Cyber.* **1979**, *9*, 62.
23. Fernandez-Fernandez, A.; Manchanda, R.; Lei, T.; Carvajal, D. A.; Tang, Y.; Kazmi, S. Z. R.; McGoron, A. J. *Mol. Imaging* **2011**, *11*, 1.